

Progress in the Modeling of NiAl-Based Alloys Using the BFS Method

Guillermo Bozzolo
Ohio Aerospace Institute
Cleveland, Ohio

Ronald D. Noebe and John Ferrante
Lewis Research Center
Cleveland, Ohio

Anita Garg
AYT Corporation
Cleveland, Ohio

Prepared for the
Second International Symposium on Structural Intermetallics
sponsored by The Minerals, Metals, and Materials Society
Champion, Pennsylvania, September 21–26, 1997



National Aeronautics and
Space Administration

PROGRESS IN THE MODELING OF NIAL-BASED ALLOYS USING THE BFS METHOD

Guillermo Bozzolo
Ohio Aerospace Institute,
Cleveland, Ohio 44142

Ronald D. Noebe, John Ferrante
National Aeronautics and Space Administration
Lewis Research Center
Cleveland, Ohio 44135

and

Anita Garg
AYT Corporation
National Aeronautics and Space Administration
Lewis Research Center
Cleveland, Ohio 44135

SUMMARY

The BFS method has been applied to the study of NiAl-based materials to assess the effect of alloying additions on structure. Ternary, quaternary and even pent-alloys based on Ni-rich NiAl with additions of Ti, Cr and Cu were studied. Two approaches were used, Monte Carlo simulations to determine ground state structures and analytical calculations of high symmetry configurations which give physical insight into preferred bonding. Site occupancy energetics for ternary and the more complicated case of quaternary additions were determined, and solubility limits and precipitate formation with corresponding information concerning structure and lattice parameter were also 'observed' computationally. The method was also applied to determine the composition of alloy surfaces and interfaces. Overall, the results demonstrate that the BFS method for alloys is a powerful tool for alloy design and with its simplicity and obvious advantages can be used to complement any experimental alloy design program.

INTRODUCTION

Development of new structural alloys and even small improvements to current alloys occur through extensive experimental trial and error, which is both costly and time consuming. However, there has been no other viable approach to alloy development, since computational methods for ternary and higher-order systems have been sorely inadequate. Although first-principles approaches are best suited for providing the most accurate and consistent framework for such studies, the complexity of the problems at hand and the overwhelming computational requirements for even simple systems, prevent these approaches from becoming useful and economical predictive tools. To date, very few calculations exist that go beyond elementary binary alloys, and even in these cases, the results are limited in scope and accuracy.

Recent developments in the area of semiempirical methods created the hope of progress in the field of alloy structure analysis and design, however, most of the methods developed in the last two decades have been severely restricted in the type and complexity of systems amenable to such studies. The purpose of these methods is to provide an efficient and accurate way to compute the total energy of arbitrary atomic systems in terms of the geometrical configuration of the atoms. In most cases, the existing techniques are restricted to a few systems for which specific (and therefore nontransferrable) parameterizations are developed, thus limiting their predictive power and overall usefulness. Recently, a new semiempirical method was developed with the goal of avoiding these limitations of existing methods, and hopefully demonstrating the usefulness of such techniques. The BFS (Bozzolo-Ferrante-Smith) method for alloys (ref. 1) is particularly designed to deal with complex systems and geometries, as it has no constraints regarding the type and number of elements under consideration, or on the number or type of resulting

phases. These are major obstacles for other techniques, which are usually limited to the treatment of a few elements, binary alloys and single phase components. Moreover, other techniques only provide reliable results for bulk properties, offering little confidence in applications such as extended defects of surfaces and interfaces (ref. 2).

The BFS method is based on quantum perturbation theory and the solution of simple transcendental equations for each atom in the sample, in order to compute its contribution to the total energy. Thus, the computational requirements are trivial (a PC was used to perform all the calculations in this paper), favoring the use of BFS for large-scale simulations. In addition, the method relies on first-principles determined parameters with general transferrability to broad situations, as opposed to competing techniques that have the additional disadvantage that their parameters or potentials have to be determined and optimized for each specific application. Thus, the method provides a simple framework for large scale simulations.

The predictive capabilities of the BFS method have been successfully tested in a number of systems (ref. 3), but most recently it has been used to predict and understand the effect of ternary alloying additions on the structure of NiAl-based alloys. Both experimental and theoretical studies were conducted in parallel, each in turn supporting the other. The experimental work was conducted in the normal course of evaluating these alloys and as a check on the modeling effort. Based on the performance of the BFS method to the basic binary and ternary systems, it has been applied to more complex systems and the modeling efforts have begun to lead the way for the alloy design program. In this paper, we will present an overview of recent results from BFS-based analyses of the structure of NiAl with ternary and quaternary additions (Ti, Cr, Cu), including a preliminary analysis of a 5-element alloy, together with conclusions drawn from extensive Monte Carlo/Metropolis large-scale computer simulations of these alloys. When appropriate, the modeling results have been compared to TEM and other experimental observations.

The BFS Method

For a given distribution of atoms, the BFS method computes the configurational energy of formation by means of a perturbation theory-based approach. Ground state structures of alloys are therefore obtained by optimizing the atomic distribution via Monte Carlo simulations (ref. 3). The number of parameters necessary for this approach are four for each single element and two for each binary combination. These are generated from first-principles linear muffin tin orbital calculations (ref. 4). For the sake of brevity, we refer the reader to previous papers on the BFS method and its application to surface studies (ref. 5) and alloy characterization (ref. 6) for further details.

The BFS method is based on the idea that the energy of formation of an alloy is the superposition of individual contributions of atoms in the alloy

$$\epsilon_i = \epsilon_i^S + g_i(\epsilon_i^C - \epsilon_i^0)$$

The two main contributions to the energy are ϵ_i^S , which is the strain energy computed with perturbation-theory based Equivalent Crystal Theory (ECT) (ref. 7), that accounts for the actual geometrical distribution of the surrounding atoms computed as if they were of the same atomic species. The energy associated with this defect i.e. the difference in atomic locations seen by the reference atom i in the alloy, and the equilibrium crystal, is represented by the strain energy. In a similar fashion the difference in composition seen by the reference atom in the alloy and the one in a monoatomic crystal can also be considered as a defect. The chemical energy $\epsilon_i^C - \epsilon_i^0$, which takes into account the different atomic species of each neighboring atom, can be represented by 'perturbing' the electronic density in the overlap region between dissimilar atoms while locating them at equilibrium lattice sites of atom i . In doing so, the calculation of the chemical energy is similar in essence to that of the strain energy. Appropriate changes must be made to account for the nature of the 'defect'. ϵ_i^0 is a reference energy computed in the same fashion as (see ref. 5), but assuming that all surrounding neighbors are of the same atomic species as the reference atom. The coupling function ensures the correct asymptotic behavior of the chemical energy term.

The implementation of the BFS method to a given system, requires the knowledge of a small number of parameters. For each individual element, four parameters are needed (cohesive energy, bulk modulus, equilibrium Wigner-Seitz radius, single vacancy formation energy). While these quantities are readily available from experiment in most cases, we rely on the results of Linear-Muffin-Tin-Orbital (LMTO) first-principles calculations, in order to

avoid problems of experimental error, inconsistency and lack of availability. For each pair of elements, two parameters are needed (for example, the heat of formation and equilibrium lattice parameter of a known ordered structure, or heats of solution in the dilute limit) which can also be easily computed using LMTO.

Reference 5 provides details on the BFS method, its implementation, the operational procedure and the approach used in the Monte Carlo/Metropolis computer simulation. Table I lists the ECT parameters for the bcc variants of the pure elements. The BFS parameters for the binary combinations of these elements used in this work are listed in table II. More details on the determination of the BFS parameters can be found in reference 8. It should be emphasized that the parameters listed in tables I and II were used to generate all the results presented in this paper, demonstrating the robust nature of this approach.

Binary Alloys—Defect Structure of B2 NiAl

A previous application of the BFS method to the analysis of the zero-temperature defect structure of NiAl alloys successfully reproduced the defect structure as a function of stoichiometry (ref. 8). This study raised confidence in the authenticity of the parameters used for the NiAl system, which once determined, remain the same for any further analysis based on this system.

Based on a 72-atom bcc cell, a few hundred atomic configurations were defined and then their energy computed using the BFS method. By creating this catalogue of possible defect structures, the lowest energy ground state configurations for each composition can be determined (if included in the catalogue) along with a series of possible metastable structures (those configurations with energies close to that of the ground state). Moreover, the site preference of the alloying additions as a function of their concentration, and as a result, information regarding the solubility limit and the possible formation of second phases, can also be obtained.

For the case of nonstoichiometric B2 NiAl, this approach indicates that Ni-rich NiAl alloys are essentially substitutional in nature, whereas Al-rich alloys are characterized by the presence of vacancies primarily in Ni but also in Al sites (ref. 8). Both results are in excellent agreement with experiment (ref. 9). The calculated lattice parameter of the lowest energy configurations for each composition reproduced the experimental results quite accurately, particularly for Ni-rich NiAl alloys (ref. 10). A similar approach was successfully used to investigate the zero temperature defect structure of FeAl alloys (ref. 11)

Ternary Alloys—Cr/Ti Addition to NiAl

The catalogue of individual atomic configurations mentioned in the previous section (see ref. 12 for a detailed description of the 200 configurations used) can be extended to include an appropriately large number of atomic distributions of a 3-element alloy. The set of configurations used in this investigation includes several hundred states covering almost every possible substitutional scheme for a wide range of concentrations, including a large variety of possible short- and long-range ordering patterns. A subset of this catalogue containing some simple configurations which correspond to possible site preference schemes is shown in figure 1. The energy of formation of these configurations, computed with the BFS method, is shown in figure 2 as an 'energy spectrum,' helping to visualize the relative probability of each possible defect.

From this set, it is seen that Ti preference for Al sites dominates, as is clear from the energy of formation values in table III. It is precisely this marked preference for Al sites that explains the ordering pattern seen already at low Ti concentrations: Ti atoms tend to locate themselves at opposite corners of the cube in the Al-sublattice, so that they always have Al atoms as second neighbors. This local ordering of Ti is indicative of Heusler formation. This trend towards Heusler ordering can be more clearly seen in figure 3, where the energy of formation of the complete catalogue of configurations, computed with BFS, is plotted against their Ti concentration. Those states characterized by Heusler ordering (circles in fig. 3) become energetically favored around 5 at. % Ti, with the energy gap between configurations with Heusler ordering and the next closest one in energy widening beyond that concentration. This information can be taken as an indirect way of determining the solubility limit of Ti (~5 percent) in NiAl. Beyond this value, Heusler precipitates form. The calculated lattice parameter of 0.5828 nm for the Ni_2AlTi phase from the $x_{\text{Ti}} = 25$ calculations is in excellent agreement with the reported experimental value of 0.5876 nm. Thus, based solely on BFS calculations, the lattice mismatch between NiAl and Ni_2AlTi is found to be 1.7 percent, very close to the 1.5 percent misfit obtained experimentally via TEM.

The results of several Monte Carlo/Metropolis simulations using BFS for the calculation of the energy are shown in figures 4 to 9. In these simulations, the atoms are given the freedom to find their minimum energy positions at any given temperature, thus giving valuable information on the ground state structure and its dependence on temperature. Starting from random distributions, the atoms in the sample switch positions—the exchange is accepted or rejected depending on temperature-dependent probability factors computed with BFS—until the lowest energy configuration is found. Figure 4 shows the results of Monte Carlo simulations for Ni-48Al-2Ti and Ni-40Al-10Ti, clearly showing the formation of Heusler precipitates at $x_{Ti} = 10$. The Monte Carlo results were obtained by slowly cooling an initially random state, in 100 K temperature steps until equilibrium (i.e. no noticeable change in formation energy) is achieved at each step. Figure 10 shows experimental results for three alloys (Ni-47Al-3Ti, Ni-45Al-5Ti and Ni-43Al-7Ti) in agreement with the theoretical predictions: The TEM micrographs shown in figure 10 clearly indicate the formation of Heusler precipitates beyond the solubility limit.

Cr additions affect the structure of NiAl somewhat differently than Ti: First of all, Cr preference for Al sites diminishes with increasing Cr concentration, instead it develops a tendency to segregate to bulk Al and Ni planes. This can be taken as a tendency towards the formation of Cr precipitates where Cr atoms occupy both types of sites in the bcc lattice. A similar analysis, using the same catalogue of atomic configurations as that used for Ti additions, shows that the solubility limit of Cr in NiAl is quite low, at 1 to 2 percent, and that beyond that concentration α -Cr precipitates form. The site preference scheme also indicates the tendency for displaced Ni atoms to form an interphase boundary between the NiAl matrix and the α -Cr precipitate in some cases. Previous work by Cotton et al. (ref. 13) has shown the low solubility of Cr in NiAl and figure 11 shows a TEM micrograph confirming the precipitation of Cr in a Ni-45Al-5Cr alloy. The ternary phase diagram confirms the BFS predictions of the formation of a three-phase alloy in the Ni-25Al-25Cr alloy, as shown in the results of a Monte Carlo/BFS simulation in figure 5. These results, together with the previous ones for Ti additions, raise the necessary confidence in the parameterization of Ni, Al, Cr and Ti to model more complicated systems. In what follows, we will investigate quaternary alloys composed of these elements concentrating on the effect of alloying interactions on site preference and their influence on the resulting microstructure of the alloy.

Quaternary Alloys

Having established the reliability of the BFS calculations based on a successful comparison with experiment for the ternary alloys, we can now exploit the transferrability of the parameters determined for Ni, Al, Cr and Ti as well as the versatility of the BFS method and use them for similar studies of 4- and 5-element alloys. The first goal is to investigate the changes in behavior of each alloying addition due to the presence of the others. By defining a catalogue of configurations contemplating most of the possible distributions of the four atomic species, we can study the site preference energetics of each alloying addition, as shown in figure 12. This figure is an 'energy spectrum' which displays the results of the energy of formation of different configurations correspond to different site substitution alternatives in the catalogue.

The site preference scheme shown in figure 12 for Cr additions to NiAl-Ti alloys shows that the preference of Ti for Al sites is still the dominant behavior. For stoichiometric NiAl+(Ti,Cr) alloys, Ti and Cr tend to substitute for Al and Ni respectively, emphasizing the weak preference of Cr for Al sites in the ternary case. The energy levels for Cr additions to Heusler (Ni_2AlTi) alloys also indicates that Cr will have little influence in altering the individual behavior of Ti. As a result, it is reasonable to expect little interaction between Ti and Cr atoms. This translates into each element retaining its individual behavior as seen in the ternary case, with Ti (depending on its concentration) forming Heusler precipitates and Cr creating α -Cr precipitates. However, the site substitution schemes also suggest some possible additional features: antistructure Ni atoms (in Al sites) and the possible creation of a Ni-rich phase due to the displaced Ni atoms. A Monte Carlo/BFS simulation of a temperature cascade for a Ni-Al-Ti-Cr alloy shown in figure 6 confirms the behavior extracted from the site preference calculations. Besides the expected formation of α -Cr and Heusler (Ni_2AlTi) precipitates, several antistructure Ni(Al) atoms and clustering of Ti atoms around these antistructure atoms is observed, as well as some indication for the formation of a Ni-film separating the NiAl phase from the Cr precipitate.

On the other hand, Cu additions to NiAl+Ti alloys display a different behavior. The site preference scheme for Cu in NiAl is similar to that of Ti in NiAl, however, Cu additions to Ni-Al-Ti alloys show a clear preference of Al sites, leading to a weak interaction between Cu and Ti atoms. Therefore, the addition of Cu and Ti to NiAl is

characterized by two mainly separate behaviors: Ti forms Heusler precipitates at about the same solubility limit as that found in ternary Ni-Al-Ti cases, and Cu is in solid solution in the NiAl matrix, with a strong preference for Al sites. This can be seen from examining figure 13, where the site preference of Cu in NiAl and NiAl+Ti alloys is shown. Figure 7 shows a Monte Carlo temperature cascade in a Ni-43Al-5Ti-2Cu alloy. The presence of Cu atoms does not alter the behavior of Ti in NiAl at low concentrations, consistent with the energy diagram shown in figures 12 and 13.

Pentalloys

While constraining the set of configurations to bcc-based structures proved to be sufficient in describing the NiAl based ternary and quaternary alloys discussed in previous sections, such a radical constraint (which, if lifted, would give information on the possible formation of additional ordered phases) might prove to be too restrictive when studying higher order systems. Any information obtained within this framework is therefore limited and should be interpreted and analyzed as such. In spite of this fact, it is still of interest to compare the behavior of alloys composed of all five elements, with respect to their behavior in the 3- and 4-element alloys. In the future, this constraint on structure will be lifted, since it is only a matter of computational efficiency and not an inherent problem with the BFS method itself.

The study of substitutional site preferences for 5-element alloys as a function of concentration is obviously much more involved than that for the simpler systems studied before, and it exceeds the scope of this paper. However, it should be noted that no additional input is required by BFS to tackle this task, as the parameters used in the 5-element alloy calculation are the same ones used in the previous examples and listed in tables I and II. Studying such fundamental issues as site preference in these higher order systems amounts to just a larger set of possible configurations with a slight increase in the computational effort involved. However, we have analyzed a 5-element alloy: Ni-22.56Al-9.47Ti-33.5Cr-1.95Cu. The concentrations were chosen so as to compare directly with the previous examples, i.e., Ti forms Heusler precipitates at that concentration, Cr forms α -Cr precipitates, with the addition of a small amount of Cu in solid solution. The results of Monte Carlo/BFS simulations shown in figure 8, display a wealth of information regarding the behavior of the five elements in such a reduced computational cell.

A basic feature in figure 8 is the formation of a NiAl matrix, dotted with Ni_2AlTi precipitates as well as the presence of α -Cr, a behavior that is not surprising in view of the results obtained for the quaternary case and the low concentration of Cu. However, something unusual is observed with the Cu atoms in the presence of Ti and Cr. In Ni-Al-Ti-Cu alloys Cu atoms favored the formation of short-range order patterns occupying Al sites in Ti-Al rich planes, but in the pentalloy, Cu tends to completely segregate to the NiAl/Cr interphase. In addition, there is evidence for the formation of a ternary phase of Ni, Al and Ti (second and third plane in fig. 8) at the interface between the NiAl matrix and the Cr precipitate. This seems to be a natural consequence of the composition studied and not just the result of one isolated simulation since the same feature has showed up repeatedly in additional simulations. While the essential features (NiAl, Ni_2AlTi , α -Cr) appear in all simulations, but in different parts of the computational cell, this new quaternary phase always forms along the interphase.

Alloy Surfaces

The BFS method has been also applied to surfaces of the alloys studied in this work, with the main goal being to establish a comparison between the bulk structure and the surface composition. While the bulk results found some experimental validation as shown in this work, the surface analyses are of a pure predictive nature. These results are discussed in detail in reference 14. As an example, figure 9 shows a comparison between the bulk and surface composition of a Ni-25Al-25Ti alloy (Heusler phase). In contrast with the bulk cell, the results of a Monte Carlo/BFS simulation of a thin film with the same composition shows the segregation of Ti and Al to the surface planes and a mostly Ni-Ti second plane, at the expense of a depletion of Ti in the bulk. Similar features are found for quaternary alloys, including the formation of ordering patterns different from those found in the bulk. The simulations shown in figure 9 correspond to free-standing thin films, where no substrate is considered. Current work on surface structure of multicomponent systems includes details on the growth process, and segregation to the interface. It is expected that the ability of the method to deal with these situations will facilitate the study of grain boundaries.

CONCLUSIONS

The results in this study represent a brief survey of the general effect of different alloying additions on the structure of NiAl. In doing so, we have subjected the BFS method to severe tests of its validity. Based on available experimental evidence, the method passed these tests both quantitatively and qualitatively. First, the correct solubility limit was predicted for both the NiAl+Ti and NiAl+Cr systems. The correct lattice parameter dependence on concentration was predicted for the NiAl+Ti system. The correct structure of the second phase particles was predicted for both cases, as well as the lattice mismatch between the alloy matrix and the precipitating phases. Site preference schemes were computed for the binary, ternary and quaternary systems studied. Based on these results, the study included predictions of the phase structure of quaternary and 5-element systems, both for their bulk and surface properties. Furthermore, we have shown that first-principles input can be used to generate needed parameters, thus removing the limitations of needing experimental data bases for input parameters.

These results show that most of the necessary parameters for a purely analytical alloy design approach are now within reach. The results also provide confidence in the BFS technique, the authenticity and transferrability of the parameters used, and the approach used for obtaining these parameters, thus the need to acquire experimental input parameters is completely eliminated by the use of the BFS method. Future applications will be focused towards integrating the role of techniques such as BFS in aiding the material design process.

ACKNOWLEDGMENTS

Fruitful discussions with Dr. N. Bozzolo are gratefully acknowledged. We would also like to thank Dr. B. Good for providing the code for performing the Monte Carlo simulations, and Dr. C. Amador for providing the input parameters for the BFS calculations.

REFERENCES

1. G. Bozzolo, J. Ferrante and J.R. Smith, Phys. Rev. B, 45 (1992) pg. 493.
2. A. Voter, MRS Bulletin, 21 (2) (1996) pg. 21.
3. G. Bozzolo, B. Good and J. Ferrante, Mat. Res. Soc. Symp. Proc., Vol. 408, pg. 1996.
4. O.K. Andersen, A.V. Postnikov and S.Y. Savrasov, Mat. Res. Soc. Symp. Proc. 253 (1992) pg. 37.
5. G. Bozzolo, J. Ferrante and R. Kobistek, J. Computer-Aided Mater. Design 1 (1994) pg. 305.
6. G. Bozzolo and J. Ferrante, J. Computer-Aided Mater. Design 2 (1995) pg. 113.
7. J.R. Smith, T. Perry, A. Banerjee, J. Ferrante and G. Bozzolo, Phys. Rev. B 44 (1991) pg. 6444.
8. G. Bozzolo, C. Amador, J. Ferrante and R.D. Noebe, Scripta Metall. Mater. 25 (1995) pg. 1907.
9. M. Kogachi, S. Minamigawa and K. Nakahigashi, Acta Metall. Mater. 40 (1992) pg. 1113.
10. R.D. Noebe, R.R. Bowman and M.V. Nathal, Int. Mater. Rev. 38 (1993) pg. 193, and references therein.
11. G. Bozzolo, J. Ferrante, R.D. Noebe and C. Amador, Scripta Mater. 36 (1997) pg. 813.
12. G. Bozzolo, R.D. Noebe, A. Garg, J. Ferrante and C. Amador, to be published.
13. J.D. Cotton, R.D. Noebe, M.J. Kaufman, Structural Intermetallics, R. Darolia et al. eds., The Minerals, Metals and Materials Society, 1993, pp. 513-523.
14. G. Bozzolo, J. Ferrante and R.D. Noebe, Surf. Sci., pp. 377-379 (1997) 1028.

TABLE I.—LMTO AND ECT PARAMETERS FOR HTE BCC-STRUCTURED VERSIONS OF THE VARIOUS ELEMENTS USED IN THIS WORK. THE FIRST-PRINCIPLES LMTO PARAMETERS ARE USED TO DETERMINE THE ECT PARAMETERS (SEE REF. 6)

LMTO results					ECT parameters			
Atom	Lattice parameter	Cohesive energy	Bulk modulus	Vacancy energy	p	α	λ	l
Ni	2.752	5.869	249.2	3.0	6	3.0670	0.763	0.2716
Al	3.192	3.942	77.3	1.8	4	1.8756	1.038	0.3695
Ti	3.213	6.270	121.0	2.0	6	2.6805	1.048	0.3758
Cr	2.837	4.981	286.0	4.9	6	2.8580	0.6460	0.2300
Cu	2.822	4.438	184.5	1.8	6	3.1082	0.7614	0.2710

TABLE II.—BFS PARAMETERS. THE ENTRY A_{ij} CORRESPONDS TO THE BFS PARAMETER Δ_{ij} . (SEE REF. 6)

j/i	Ni	Al	Ti	Cr	Cu
Ni	0.00000	-0.05813	-0.06582	-0.02975	0.02085
Al	0.08220	0.00000	-0.06360	-0.01307	0.05887
Ti	0.45690	0.22830	0.00000	0.06579	0.21964
Cr	0.20480	-0.01637	-0.04691	0.00000	0.02664
Cu	-0.01489	-0.04793	-0.055555	-0.01016	0.00000

TABLE III.—ENERGY OF FORMATION AND LATTICE PARAMETER FOR THE DEFECT STRUCTURES SHOWN IN FIGURE 1 FOR TWO Ti CONCENTRATIONS. THE SUBINDEXES INDICATE THE DISTANCE BETWEEN THE TWO DEFECTS. FOR EXAMPLE, $\text{Ti}(\text{Ni})\text{Al}+\text{Ti}(\text{Al})_{\text{NN}}$ INDICATES THAT THE ANTISTRUCUTRE Ni ATOM AND THE Ti ATOM IN THE Al SITE ARE NEAREST-NEIGHBORS (NN)

x_{Ti}	Description of the configuration	Energy of formation, eV/atom	Lattice parameter, Å
1.39	$\text{Ti}(\text{Ni})\text{Al}_{\text{NN}}$	-0.41320	2.870
	$\text{Ti}(\text{Ni})\text{Al}_{\text{far}}$	-0.38052	2.870
	$\text{Ti}(\text{Al})$	-6.0839	2.853
	$2\text{Ti}(\text{Ni})_{\text{NN}} + 2\text{Ni}(\text{Al})_{\text{NN}}$	-0.32607	2.881
	$2\text{Ti}(\text{Ni})\text{Al}_{\text{NN}}$	-0.32873	2.882
2.78	$\text{Ti}(\text{Ni})\text{Al}+\text{Ti}(\text{Al})$	-0.36893	2.879
	$\text{Ti}(\text{Ni})\text{Al}+\text{Ti}(\text{Al})_{\text{far}}$	-0.37773	2.878
	$2\text{Ti}(\text{Al})_{\text{NN}}$	-0.59918	2.859
	$2\text{Ti}(\text{Al})_{\text{far}}$	-0.63500	2.858
	$2\text{Ti}(\text{Al})_{\text{Heuster}}$	-0.60350	2.858

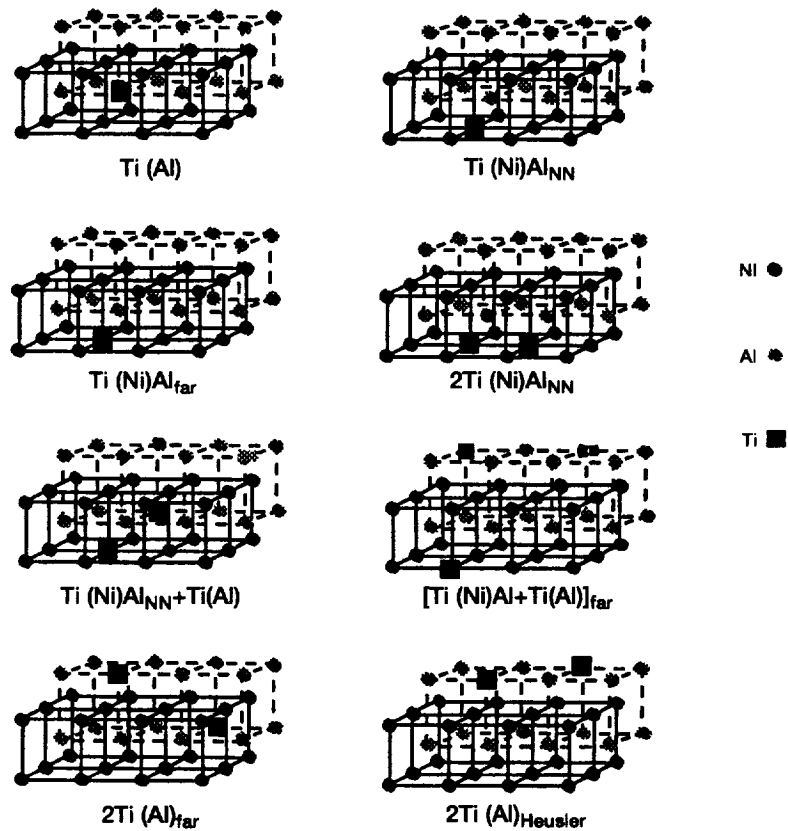


Figure 1.—Computational cells showing different substitutional schemes for Ti in NiAl. The corresponding energies of formation and lattice parameter are shown in Fig. 2 and Table 3. A(B) describes a configuration where an A atom occupies a site in the B-sublattice. A(B)C is the superposition of two substitutional defects: A(B)+(B)C. The subindices NN, far and Heusler indicate that the substitutional atoms are either at nearest-neighbor distance, at distance greater than nearest-neighbor distance or located following Heusler ordering (in opposite corners of the cube in the same sublattice).

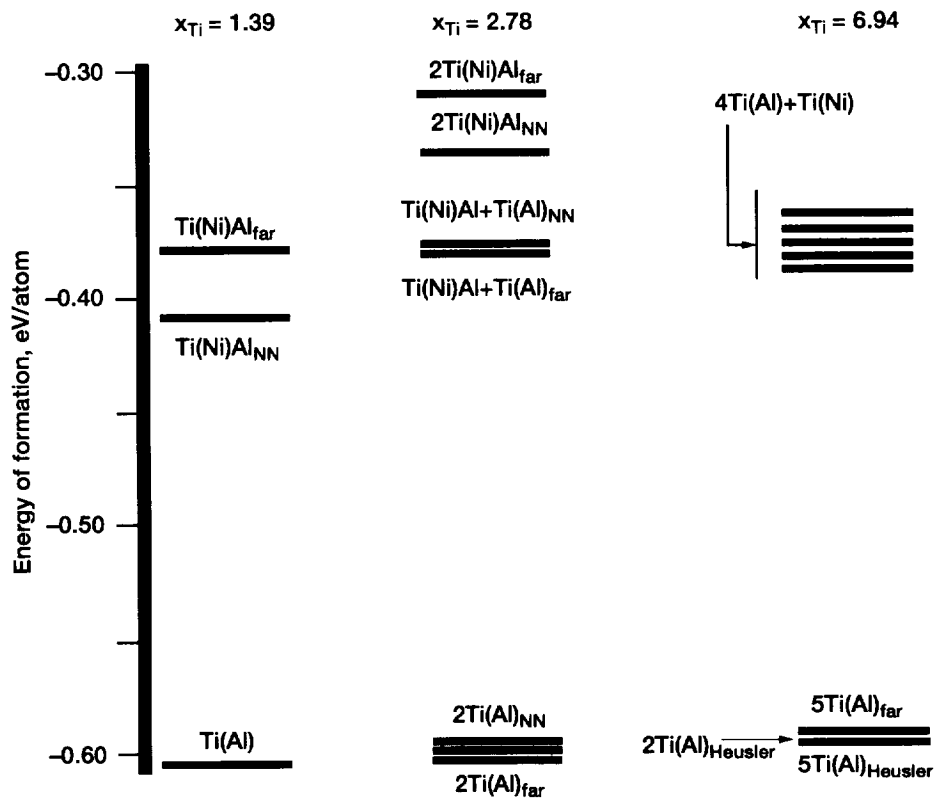


Figure 2.—Site preference energy spectrum for Ni-Al-Ti alloys. A(B) indicates an atom A in a B site and A(B)C indicates an A atom in a B site, with the B atom in a C site. See text for details.

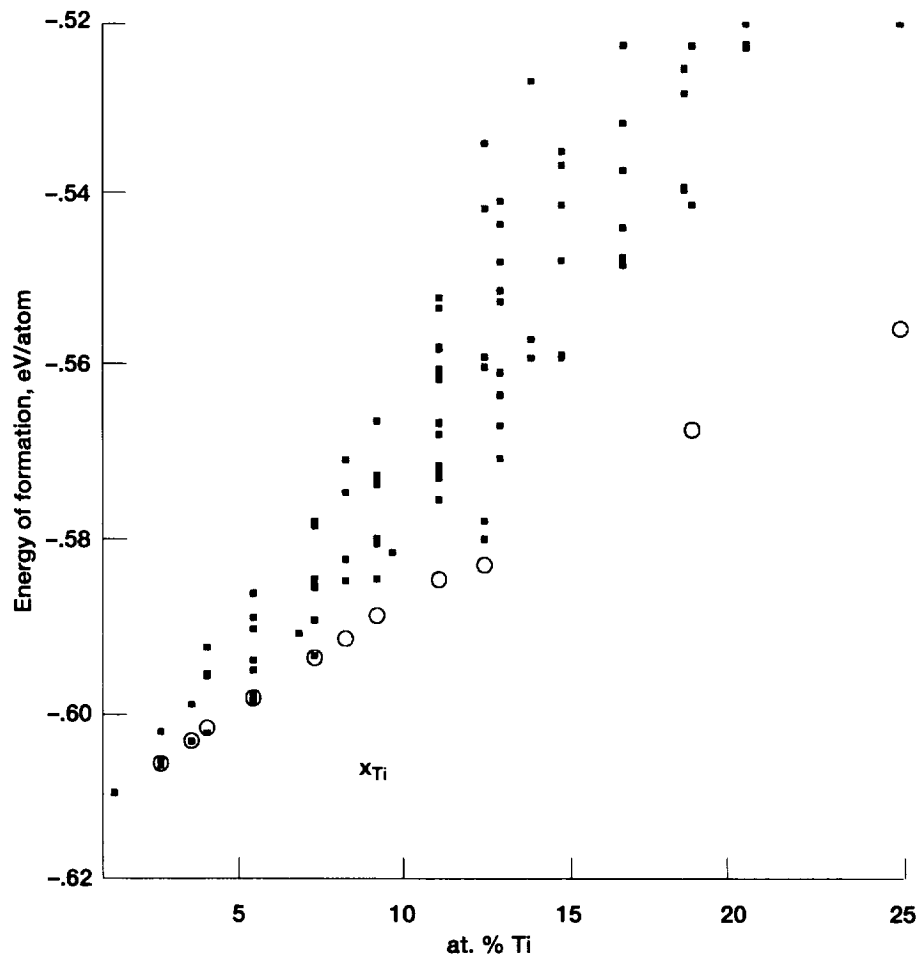


Figure 3.—Energy of formation of a large number of $\text{Ni}_{50}(\text{Al}_{50-x}\text{Ti}_x)$ bcc-based configurations (defined in Appendix 2 of Ref. 12), displaying a variety of short-range order patterns as well as completely disordered states. Those configurations characterized by Heusler ordering are denoted with open circles, whereas the solid squares indicate any other arrangement.

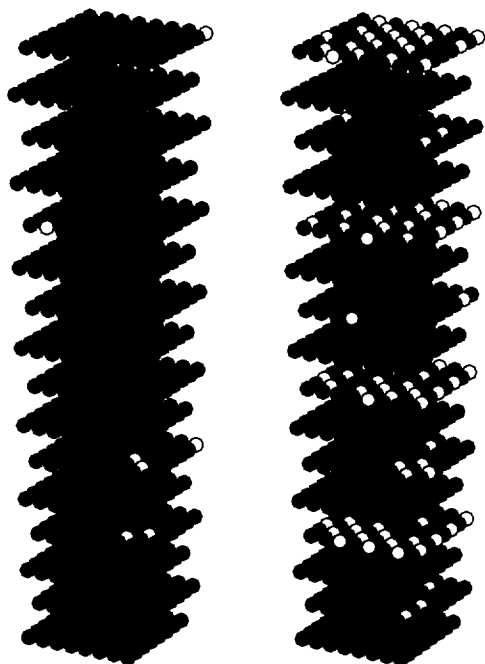


Figure 4.—Monte Carlo/BFS/Metropolis results of temperature cascade simulations of Ni-48Al-2Ti and Ni-40Al-10Ti alloys. The computational cells contains 1024 atoms and both simulations used a random placement of atoms to represent the initial, high temperature state (Ni: red; Al: blue; Ti: yellow).

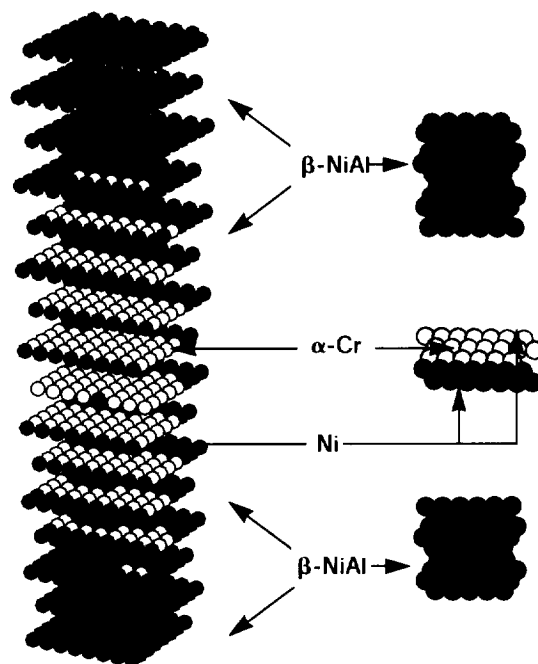


Figure 5.—Monte Carlo/BFS/Metropolis results of temperature cascade simulation for a Ni-25Al-25Cr alloy (Ni: red; Al: blue; Cr: yellow circles) The computational cells contains 1024 atoms. The initial state corresponded to a completely random state, while the room temperature alloy consists of three phases: NiAl, α -Cr, and a Ni-rich phase, consistent with the ternary phase diagram.

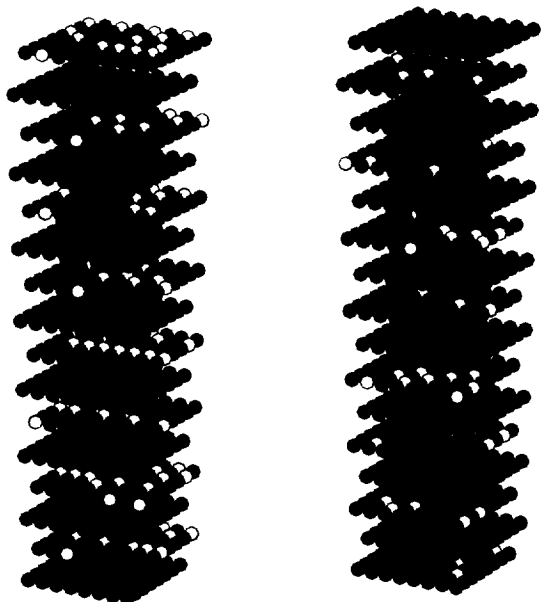


Figure 6.—Monte Carlo results of a temperature cascade on a Ni-23Al-10Ti-34Cr alloy (Ni: red; Al: blue; Ti: yellow; Cr: green).

Figure 7.—Monte Carlo results of a temperature cascade on a Ni-43Al-5Ti-2Cu alloy (Ni: red; Al: blue; Ti: yellow; Cr: green).

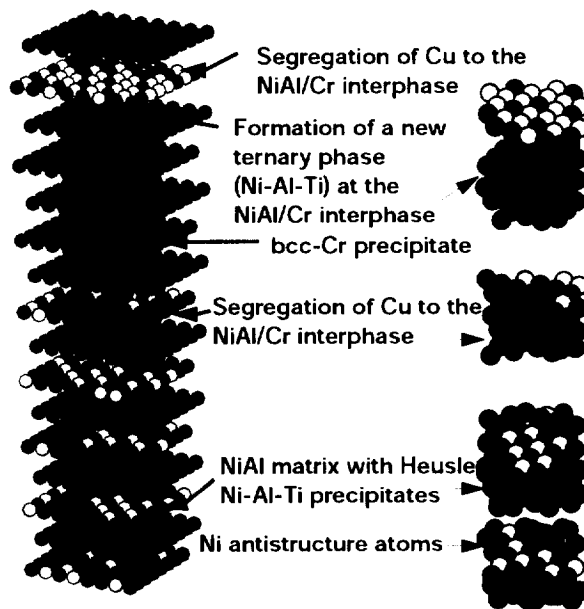


Figure 8.—Monte Carlo results of temperature cascade on a Ni-22.56Al-9.47Ti-33.5Cr-1.95Cu alloy, showing the final state at 300 K. Ni, Al, Ti Cr and Cu are represented with red, blue, yellow, green and black circles, respectively.

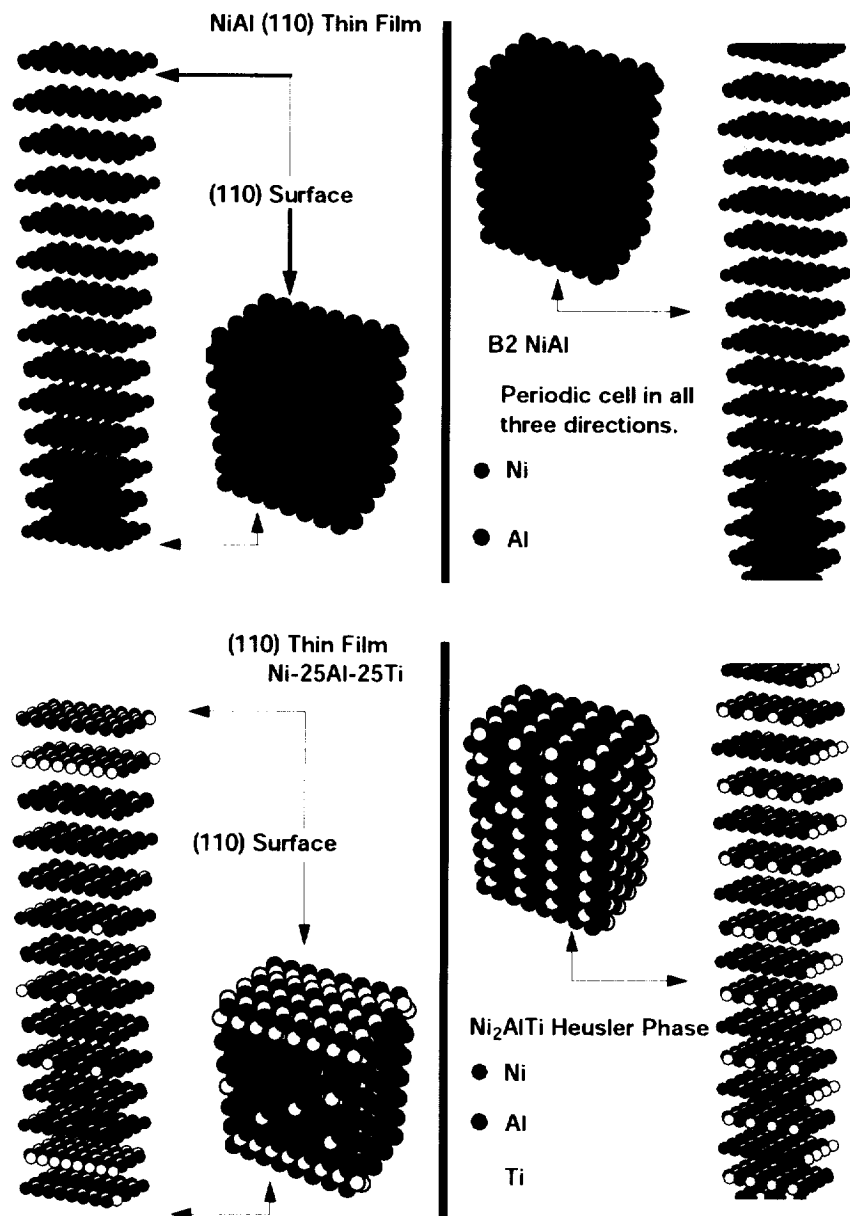


Figure 9.—Comparison of bulk and thin film compositions for NiAl (top) and Ni₂AlTi (bottom) alloys. The thin film cells are periodic in two directions, perpendicular to the top and bottom planes. The bulk cell is periodic in all three directions. The free-standing thin film terminates in two (100) surfaces.

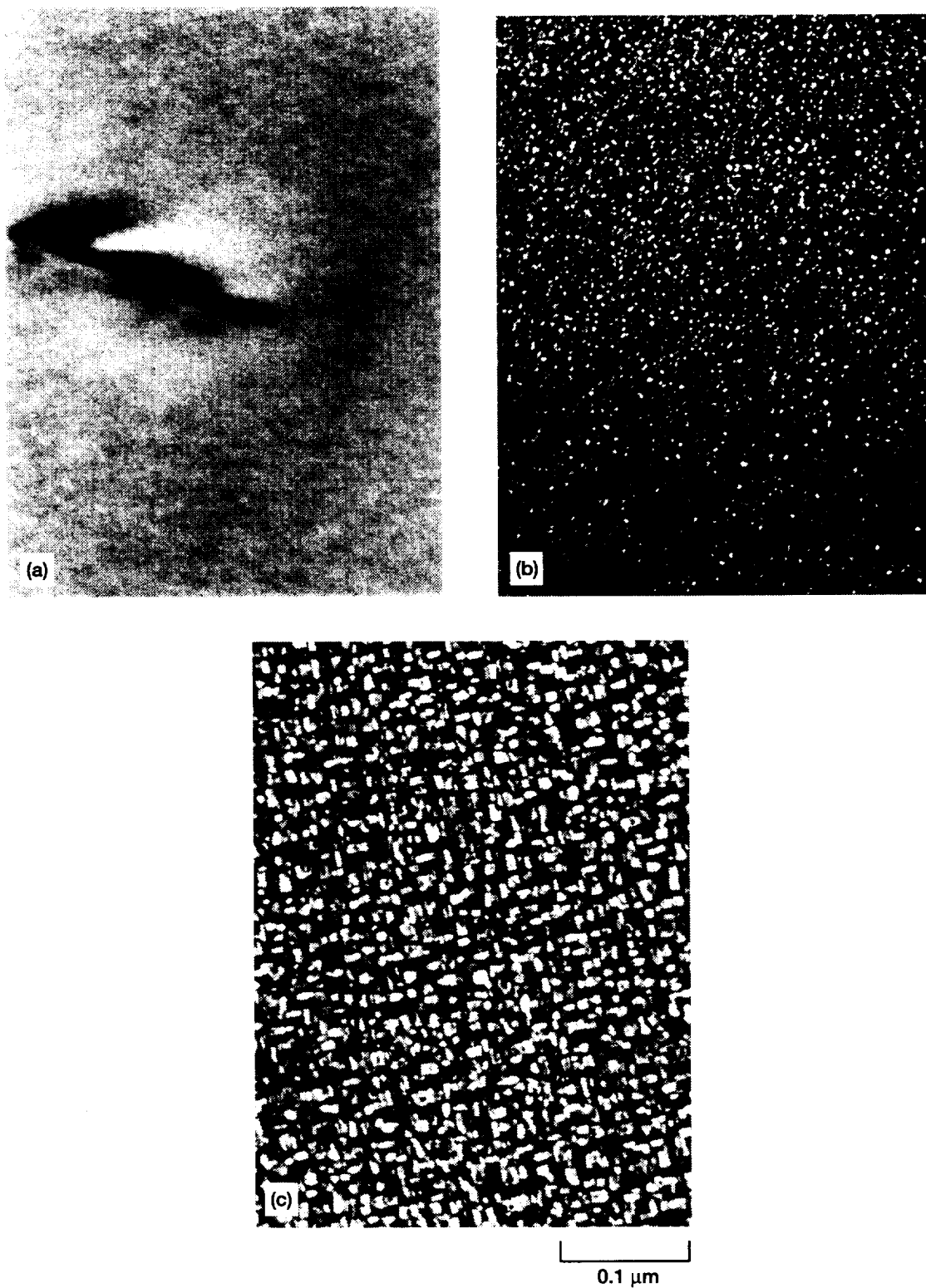


Figure 10.—TEM images of (a) a precipitate-free Ni-47Al-3Ti alloy, (b) precipitation of fine Heusler particles in a Ni-45Al-5Ti alloy and (c) dense precipitation of rectangular shaped Heusler particles in a Ni-43Al-7Ti alloy.

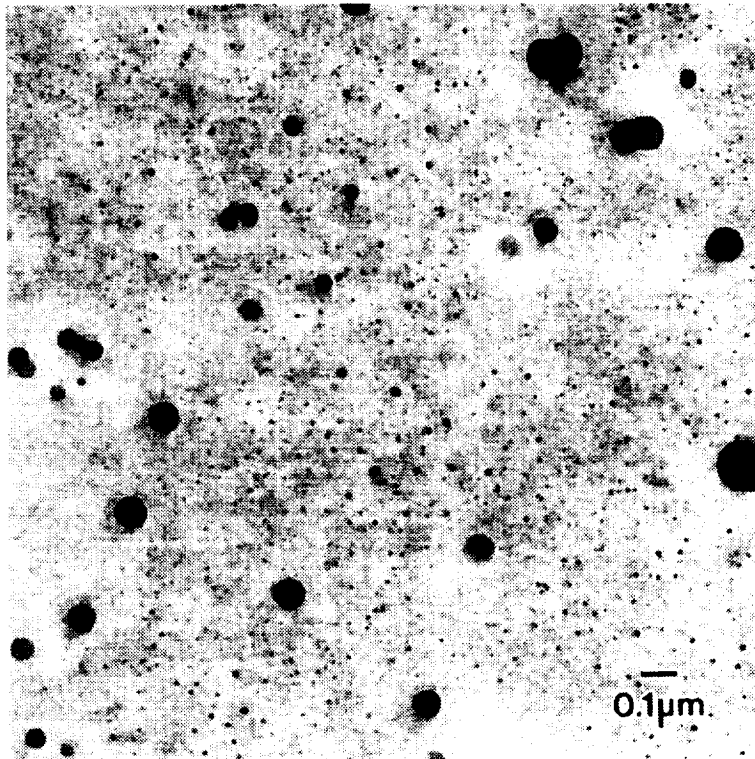


Figure 11.—TEM micrograph of Ni-45Al-5Cr, showing α -Cr precipitates in a β -NiAl matrix.

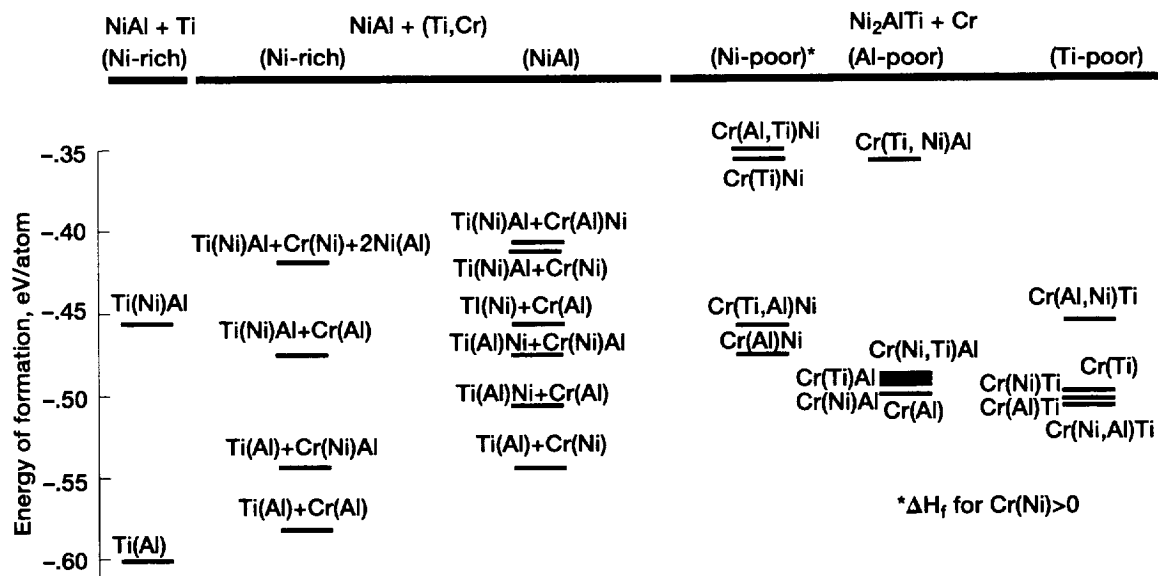


Figure 12.—Site preference 'energy spectrum'. Each line corresponds to the energy of formation of a given configuration characterized by the substitutional defect indicated. The different columns correspond to 1) Ti additions to Ni-rich NiAl alloys, 2) Ti and Cr additions to Ni-rich NiAl alloys and 3) stoichiometric NiAl alloys. Columns 4-6 correspond to Cr additions to Ni-, Al- and Ti-poor Ni₂AlTi alloys respectively.

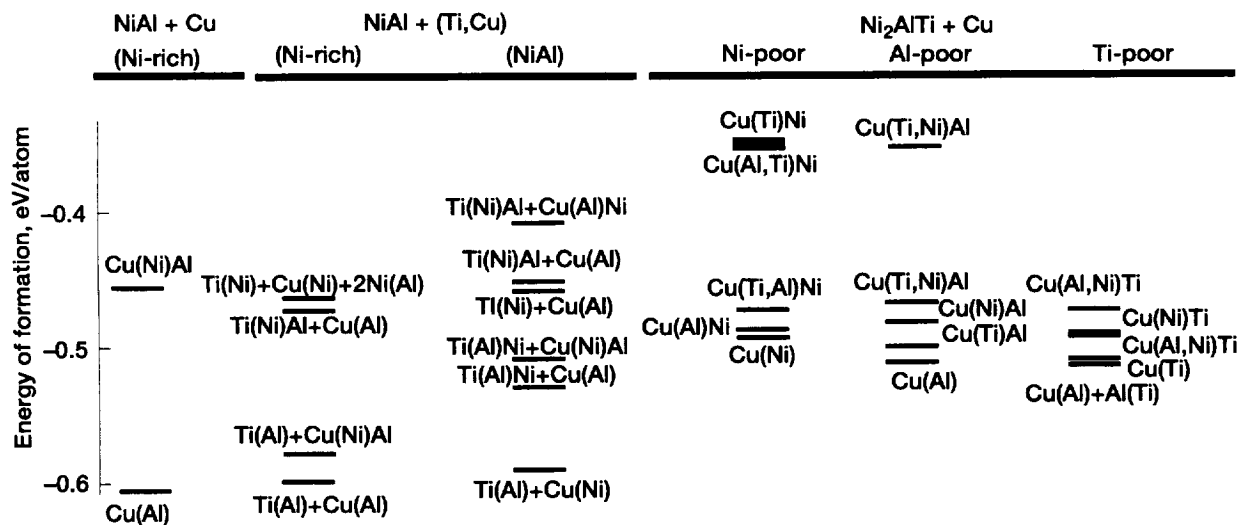


Figure 13.—Site preference 'energy spectrum' for Ni-Al-Ti-Cu alloys. Each line corresponds to the energy of formation of a given configuration characterized by the substitutional defect indicated. Several cases are considered: Ti additions on Ni-rich alloys (first column), Ti and Cu additions to Ni-rich (second column) and stoichiometric (third column) NiAl alloys. Several cases of Cu additions to Heusler Ni₂AlTi alloys are shown in the last three columns.

REPORT DOCUMENTATION PAGE			Form Approved OMB No. 0704-0188	
Public reporting burden for this collection of information is estimated to average 1 hour per response, including the time for reviewing instructions, searching existing data sources, gathering and maintaining the data needed, and completing and reviewing the collection of information. Send comments regarding this burden estimate or any other aspect of this collection of information, including suggestions for reducing this burden, to Washington Headquarters Services, Directorate for Information Operations and Reports, 1215 Jefferson Davis Highway, Suite 1204, Arlington, VA 22202-4302, and to the Office of Management and Budget, Paperwork Reduction Project (0704-0188), Washington, DC 20503.				
1. AGENCY USE ONLY (Leave blank)		2. REPORT DATE September 1997		3. REPORT TYPE AND DATES COVERED Technical Memorandum
4. TITLE AND SUBTITLE Progress in the Modeling of NiAl-Based Alloys Using the BFS Method			5. FUNDING NUMBERS WU-523-22-13-00	
6. AUTHOR(S) Guillermo Bozzolo, Ronald D. Noebe, John Ferrante, and Anita Garg				
7. PERFORMING ORGANIZATION NAME(S) AND ADDRESS(ES) National Aeronautics and Space Administration Lewis Research Center Cleveland, Ohio 44135-3191			8. PERFORMING ORGANIZATION REPORT NUMBER E-10875	
9. SPONSORING/MONITORING AGENCY NAME(S) AND ADDRESS(ES) National Aeronautics and Space Administration Washington, DC 20546-0001			10. SPONSORING/MONITORING AGENCY REPORT NUMBER NASA TM-113117	
11. SUPPLEMENTARY NOTES Prepared for the Second International Symposium on Structural Intermetallics sponsored by The Minerals, Metals, and Materials Society, Champion, Pennsylvania, September 21-26, 1997. Guillermo Bozzolo, Ohio Aerospace Institute, 22800 Cedar Point Road, Cleveland, Ohio 44142; Ronald D. Noebe and John Ferrante, NASA Lewis Research Center; Anita Garg, AYT Corporation, 21000 Brookpark Rd., Cleveland, Ohio 44135. Responsible person, Guillermo Bozzolo, organization code 5140, (216) 433-5824.				
12a. DISTRIBUTION/AVAILABILITY STATEMENT Unclassified - Unlimited Subject Categories 61, 76, and 26 This publication is available from the NASA Center for AeroSpace Information, (301) 621-0390.			12b. DISTRIBUTION CODE	
13. ABSTRACT (Maximum 200 words) The BFS method has been applied to the study of NiAl-based materials to assess the effect of alloying additions on structure. Ternary, quaternary and even pent-alloys based on Ni-rich NiAl with additions of Ti, Cr and Cu were studied. Two approaches were used, Monte Carlo simulations to determine ground state structures and analytical calculations of high symmetry configurations which give physical insight into preferred bonding. Site occupancy energetics for ternary and the more complicated case of quaternary additions were determined, and solubility limits and precipitate formation with corresponding information concerning structure and lattice parameter were also 'observed' computationally. The method was also applied to determine the composition of alloy surfaces and interfaces. Overall, the results demonstrate that the BFS method for alloys is a powerful tool for alloy design and with its simplicity and obvious advantages can be used to complement any experimental alloy design program.				
14. SUBJECT TERMS Alloys; Semiempirical methods; Computer simulations; Intermetallics			15. NUMBER OF PAGES 17	
			16. PRICE CODE A03	
17. SECURITY CLASSIFICATION OF REPORT Unclassified	18. SECURITY CLASSIFICATION OF THIS PAGE Unclassified	19. SECURITY CLASSIFICATION OF ABSTRACT Unclassified	20. LIMITATION OF ABSTRACT	